The removal efficiency and long-term hydraulic behaviour of zero valent iron/lapillus mixtures for the simultaneous removal of Cu 2+ , Ni 2+ and Zn 2+

The removal efficiency and long-term hydraulic behaviour of zero valent iron/lapillus mixtures for the simultaneous removal of Cu^{2+}, Ni^{2+} and Zn^{2+}

Stefania Bilardi *, Paolo Salvatore Calabrò *, Nicola Moraci *

*Department of Civil, Energy, Environment and Materials Engineering (DICEAM), Mediterranea University of Reggio Calabria, Reggio Calabria, Italy

Abstract

Granular mixtures composed of zero valent iron (ZVI) and lapillus at two different weight ratios (i.e. 30:70 and 50:50) were tested through column experiments for the simultaneous removal of Cu^{2+}, Ni^{2+} and Zn^{2+} present in aqueous solutions at high concentrations. The results were used to evaluate the feasibility of the above-mentioned granular mixtures as reactive media in permeable reactive barriers (PRB) for the remediation of groundwater polluted by metals. Test results showed that the two granular reactive media efficiently removed the three heavy metals under study according to the following removal sequence Cu>Zn>Ni. The granular mixture with the higher iron content showed a proportionally higher removal rate but also a higher reduction of hydraulic conductivity over time. Different removal mechanisms occurred for the three contaminants in question. Considering that for Ni and Zn the main removal mechanism was probably adsorption, we used different mathematical models, in order to predict the breakthrough curves for the adsorption mechanisms. The Adams-Bohart model showed the best fit with the experimental data and it was thus used to predict the zinc removal front within the barrier thickness. Finally, we showed that the mathematical approach may be used for the design of PRBs for the reactive media and contaminants used in this research.

Keywords: Adsorption, groundwater remediation, heavy metals, breakthrough curve, modelling, column test.

Corresponding author: Prof**.** Nicola Moraci

Department of Civil, Energy, Environment and Materials Engineering (DICEAM), Mediterranea University of Reggio Calabria, Via Graziella loc. Feo di Vito 89122, Reggio Calabria, Italy, tel: +39 09651692263 e-mail: nicola.moraci@unirc.it

1. Introduction

The presence of heavy metals in groundwater is a serious threat to human health and the natural environment. Possible sources of pollution by heavy metals are the spilling of these substances from industries, uncontrolled landfills, mine drainages or road infrastructures.

The technology of permeable reactive barriers (PRB) is considered the most suitable solution, among the groundwater remediation technologies known to date for the removal of heavy metals, to remediate flowing groundwater (Hashim et al., 2011), also considering its environmental sustainability. Indeed, a PRB is "an emplacement of reactive media in the sub-surface designed to intercept a contaminated plume, provide a flow path through the reactive media, and transform the contaminant(s) into environmentally acceptable forms to attain remediation concentration goals downgradient of the barrier", as defined by (USEPA, 1989).

The reactive medium can either be placed into a diaphragm installed perpendicularly to the groundwater flow in order to intercept the entire plume (continuous barrier) or it can be placed between two impermeable elements, which direct the flow through it (configuration funnel and gate), or even in a caisson where the flow through the reactive medium is upward (caisson configuration) rather than horizontal, as in the two previous configurations (EPA, 1999).

A PRB can be used for the remediation of different types of contaminants by choosing the most appropriate reactive medium according to cases.

As reported in the literature, the reactive medium most largely used is the granular zero valent iron (ZVI), which can be successfully used for different organic and inorganic contaminants (Cundy et al., 2008) (Fu et al., 2014). In particular, it can immobilise a large number of heavy metals by activating several mechanisms, like redox reactions, precipitation and sorption processes (Noubactep, 2013). However, the corrosion products of ZVI, being expansive, as well as the co-precipitates and gases formed during the process can cause the clogging of the PRB pores, reducing its permeability over time and therefore its lifetime (Moraci et al., 2016a) (Moraci et al., 2016b).

74 The latter is defined as the time at which a PRB keeps adequate levels of reactivity, necessary to
75 treat contaminants at the design levels, and of hydraulic conductivity in relation to the hydraulic
76 characteristics of the aquifer.
77 A granular reactive medium derived by the combination of different materials has already been
78 proposed in order to increase the long-term performance of the barrier, by improving its long-term
79 permeability, by providing multiple mechanisms for the removal of contaminants and/or by
80 reducing costs of using single/pure granular materials (Moraci et al., 2011) (Obiri-Nyarko et al.,
81 2014). For example, as results from the literature, pure granular ZVI can be mixed with different
82 granular materials, such as sand (Bartzas and Komnitsas, 2010) (Komnitsas, 2007), pumice (Moraci
83 and Calabrò, 2010) and lapillus (Bilardi et al., 2018) (Madaffari et al., 2017) at various weight
84 ratios (w.r) to improve its long-term permeability.
85 In most studies the reactive materials were tested for the removal of single contaminants and only a
86 handful of studies have dealt with the removal of metals from multi-metal contaminated solutions.
87 However, in real conditions often more than one metal is present in the contaminated groundwater
88 so that possible interactions and competitions may occur. We thus tested here two granular mixtures
89 composed of granular ZVI and lapillus at two different w.r. (i.e. 30:70 and 50:50) for the
90 simultaneous removal of Cu^{2+}, Ni^{2+} and Zn^{2+} present in aqueous solutions at high concentrations.
91 The ZVI/lapillus granular mixtures have already been previously tested by the authors in other
92 works for the removal of nickel (Bilardi et al., 2018) (Madaffari et al., 2017) and of zinc (Bilardi et
93 al., 2018) in single metal contaminated solutions. The batch tests carried out on the pure granular
94 lapillus showed its reactivity towards zinc and nickel (Bilardi et al., 2018), whereas, column tests
95 showed that lapillus was a suitable admixing agent for granular ZVI since it allowed both the
96 optimization of the use of ZVI and the preservation of its hydraulic conductivity over time
97 (Madaffari et al., 2017). Compared to pumice, which was already proposed by the same research
98 group, lapillus has the advantage of being an undesired by-product of pumice extraction with little
99 economic value.

100 Different mechanisms were shown to be involved in the removal of the three contaminants
101 proposed in this study. In particular, copper removal was attributed to a cementation process, which
102 occurred at the ZVI surface when it was not covered by iron (hydr)oxides, which prevented electron
103 transfer (Bilardi et al., 2015) (Komnitsas, 2007). Alternatively, copper was quantitatively removed,
104 as can happen for nickel and zinc, by precipitation mechanisms (heavy metals can precipitate as
105 hydroxide when the pH of the water flowing through the ZVI substantially increases), by co-
106 precipitation with iron hydroxides or adsorption onto the (hydr)oxide surfaces (Bilardi et al., 2013).
107 As evidenced in our previous work (Bilardi et al., 2018), lapillus can slightly contribute to the
108 removal of heavy metals by adsorption on its surface (including pores) also thanks to the presence
109 of iron oxides (Bilardi et al., 2018).
110 In order to obtain information useful for the design of PRBs, in this paper we first compared the two
111 above-mentioned mixtures in terms of reactivity and hydraulic behaviour and then applied different
112 mathematical models in order to predict the evolution of the reactive behaviour of the two mixtures.
113

114 **2. Materials and Methods**

115

116 *2.1 Materials*

117 The granular ZVI was purchased from Pometon S.P.A. (Mestre, Italy) and was type FERBLAST RI
118 850/3.5, while the lapillus was purchased from SEM ‘‘Societa` Estrattiva Monterosi” s.r.l. (Viterbo,
119 Italy). As described in detail in our previous study (Madaffari et al., 2017), ZVI is mainly composed
120 of iron (>99.74% mass), with a small percentage of other identified impurities, such as Mn (0.26%),
121 O, S and C; lapillus, instead, mainly consists of silica (SiO_2, 47% mass) and oxides of various
122 elements (Al_2O_3, 15%; K_2O, 8%; Na_2O, 1%; Fe_2O_3-FeO, 7– 8%; MnO, 0.15%; MgO, 5.5% and
123 CaO, 11%). The two materials are characterised by a uniform grain size distribution; the mean grain
124 size (d_{50}) is approximately 0.5 mm and 0.4 mm for ZVI and lapillus, respectively (Madaffari et al.,
125 2017). For ZVI the specific surface area value, derived from its grain size distribution and under the

126 hypothesis of spherical particles, has been calculated equal to 0.0017 m^2/g.

127

128 *2.2 Chemicals and analytical method*

129 The contaminated aqueous solution was prepared by dissolving appropriate amounts of nickel (II)
130 nitrate hexahydrate (purity 99.999), zinc (II) nitrate hexahydrate (purity 99.999) and copper (II)
131 nitrate hydrate (purity 99.999), obtained from Sigma-Aldrich (Germany) in distilled water in order
132 to obtain a concentration of 50 mg/l for both nickel and zinc and 500 mg/l for copper. The pH of the
133 influent solution was equal to 5.
134 The concentration of Cu, Ni and Zn in the aqueous samples collected during the column tests was
135 measured using ICP-OES (Perkin Elmer OPTIMA 8000).

136

137 *2.3 Column experiments*

138 The columns used in the experiments (Figure 1) were made of polymethyl methacrylate (PMMA—
139 Plexiglas^{TM}) with a length of 50 cm and internal diameter of 5 cm. The columns were equipped with
140 six sampling ports located at different distances from the inlet (i.e., at 3, 8, 18, 28, 38 and 50 cm).
141 The columns were fed with the contaminated solution, under constant upward flow, by means of a
142 peristaltic pump (Watson Marlow 205S) using a flow rate of 0.5 mL/min (Darcy velocity equals to
143 0.38 m/day). The two materials making up the mixtures were mixed at a prefixed weight ratio (w.r.)
144 equals to 30:70 or 50:50 and the two columns were filled in layers in order to obtain a specimen as
145 homogenous as possible. The column tests, which were performed at room temperature (20 ± 3 °C),
146 were flushed with the contaminated solution from the beginning of the test.
147 The hydraulic performance of the reactive materials was studied by permeability tests, which were
148 carried out during the column tests using the falling-head or constant-head methods (Bilardi et al.,
149 2018).

150

151

152 *2.4 Analysis of column test results*

153 Column tests results were interpreted by means of the breakthrough curves. These curves were
154 obtained by plotting C_t/C_0 (contaminant concentration of the effluent/initial contaminant
155 concentration) versus operation time.

156 The breakthrough time t_b was set as the time corresponding to the first time when the contaminant
157 concentration of the effluent exceeded the regulatory limit.

158 The total mass of contaminant removed q_{tot} (mg) was calculated by equation 1:

159 $$q_{tot} = \frac{Q}{1000} \int_{t=0}^{t=t_{total}} (C_0 - C_t) \cdot dt \qquad [1]$$

160 where the new symbols Q (mL/h) and t_{total} are the flow rate and the total flow time (test duration) of
161 the column (h), respectively. In equation 1 the contaminant concentration was expressed in mg/L.

162 The equilibrium removal capacity (q_e mg/g) was calculated as follows (Eq. 2):

163 $$q_e = \frac{q_{total}}{m} \qquad [2]$$

164 where m is the dry mass of the reactive medium packed in the column (g).

165 Different mathematical models were then used in order to describe the breakthrough curves
166 obtained by the experimental data. The use of a mathematical model allows to i) identify the
167 possible reaction mechanisms involved in column systems, ii) predict the reactive behaviour of the
168 material and iii) obtain parameters useful for technology design (Moraci et al., 2017) (Sulaymon et
169 al., 2015).

170 The mathematical models used in this research to simulate the adsorption capacity of the granular
171 medium were the Thomas, the Adams-Bohart and the modified dose-response models. These
172 models, widely used in the literature to estimate the adsorptive capacity of the reactive medium (de
173 Franco et al., 2017) (Huang et al., 2017) (Mikhaylov et al., 2018) (Shanmugam et al., 2016) (Singh
174 et al., 2017), are considered semi-analytical approximation solutions of the one-dimensional
175 transport of mass of a reactive dissolved contaminant in a saturated porous medium.

176 The Thomas model (Thomas, 1948) assumes that the adsorption rate obeys to a pseudo-second-
177 order Langmuir equation with no axial dispersion in the column. It is described by the following
178 equation:

179 $$\frac{C_t}{C_0} = \frac{1}{1+\exp\left[\left(\frac{k_{Th}q_{Th}m}{Q}\right)-k_{Th}C_0t\right]} \qquad [3]$$

180 where k_{Th} is the Thomas rate constant (L/ (mg·h)), q_{Th} represents the model predicted adsorption
181 capacity (mg/g) and Q is the flow rate expressed in L/h.
182 The Adams-Bohart model (Bohart and Adams, 1920) is used to fit the first part of the breakthrough
183 curve until the concentration of the effluent reaches 15% of the inlet concentration (Huang et al.,
184 2017) (Sulaymon et al., 2015). The equation can be expressed as follows:

185 $$\frac{C_t}{C_0} = \exp\left(K_{AB.}C_0t - K_{AB}N_0\frac{T}{v}\right) \qquad [4]$$

186 where K_{AB} is the Adams–Bohart model constant (L/(mg·h)), N_0 is the sorption capacity of the
187 reactive medium by the Adams–Bohart model (mg/L), T is the medium thickness (m) and v is the
188 flow rate (m/h).
189 The modified dose-response model or Yan model (Yan et al., 2001) was proposed in order to
190 minimise the error resulting from the use of the Thomas model, especially at very small and very
191 large operation times (de Franco et al., 2017). The model can be expressed by the following
192 equation:

193 $$\frac{C_t}{C_0} = 1-\frac{1}{1+\left(\frac{C_0Qt}{q_{mdr}m}\right)^a} \qquad [5]$$

194 where q_{mdr} is the predicted adsorption capacity by the modified dose-response model (mg/g), a is
195 the kinetic constant of the modified dose-response model and Q is the flow rate expressed in L/h.
196
197

198 **3. Results and Discussion**

199

200 *3.1 Removal behaviour of ZVI/lapillus granular mixtures*

201 The results show that both mixtures were efficient in simultaneously removing the three
202 contaminants according to the following sequence: Cu>Zn>Ni (Fig. S1). This sequence may be
203 attributed to the affinity that iron hydroxides and oxides (e.g. goethite, magnetite) have for the three
204 contaminants (Bilardi et al., 2013)(Lin et al., 2017). Copper was completely removed by the two
205 mixtures for the entire duration of the tests, while the removal of nickel and zinc was limited over
206 time. Moreover, the more efficient removal of zinc compared to nickel may also be attributed to
207 lapillus, which has a higher sorption affinity for zinc than for nickel (Bilardi et al., 2018).
208 We compared the two granular mixtures considering (a) the same thickness, i.e. the same distance
209 from the column inlet (Fig. 2 and Fig. S2), and (b) the same ZVI mass (Fig. 3).
210 Figure 2 shows the normalized concentration (C/C_0), calculated at 3 cm from the column inlet, for
211 nickel (Fig. 2a), zinc (Fig. 2b), and copper (Fig. 2c), as function of time (breakthrough curves). Ni
212 removal was almost similar for the two mixtures (Fig. 2a), whereas the 50:50 mixture was shown to
213 be more efficient than the 30:70 mixture in terms of Zn and Cu removal (Fig. 2 b-c). In fact, for the
214 30:70 granular mixture the Cu breakthrough was observed at 3 cm only after 1272 h (considering a
215 regulatory limit of 1 mg/l as indicated by Italian regulation).
216 The masses of lapillus and ZVI and the breakthrough time (t_b) observed for Ni and Zn are
217 summarised in Table 1 for each sampling port. The breakthrough time was obtained considering a
218 regulatory limit of 0.02 mg/l for Ni and 3 mg/l for Zn, as indicated by Italian regulation (President
219 of the Italian Republic, 2006). Clearly, the breakthrough time increases with the thickness of the
220 reactive medium. For a thickness of 3 cm and for Ni removal the typical breakthrough curve (Fig.
221 2a) was not observed because most probably the residence time (i.e. the time that the contaminated
222 groundwater is in contact with the reactive medium) was insufficient to remove the contaminant
223 under the Italian regulatory limit. At a thickness of 3 cm, the mass of lapillus was almost similar

between the two mixtures, thus the more efficient behaviour of the 50:50 mixture was due to the ZVI mass, which was twice the amount of ZVI contained in the 30:70 mixture.

The breakthrough curves, obtained at 28 and 50 cm from the column inlet, for nickel and zinc and for the two mixtures, are shown in Figure S2. Tests results relative to copper removal are not shown since copper was completely removed from the two mixtures, at the thickness considered.

The 50:50 mixture was shown again to have a more efficient removal behaviour than the 30:70 mixture, both at 28 cm (Fig. S2a-b) and at 50 cm (Fig. S2c-d) from the column inlet. This behaviour was likely due to ZVI mass, which, as previously observed, was almost twice the mass of ZVI contained in the 30:70 mixture, highlighting the importance of ZVI content per unit volume of the column.

The second comparison between the 30:70 and 50:50 granular mixtures is depicted in Figure 3 where the two mixtures were compared for nickel and zinc removal considering a similar amount of ZVI mass but at different reactive medium thicknesses (Table 1). Cu results are again not shown since it was almost completely removed at the thicknesses considered and no difference between the two mixtures was observed.

The behaviour of the two reactive media was very similar at low ZVI masses (Fig. 3 a-b), i.e. with a ZVI mass equals to 172.8 g or 154 g for the 30:70 and 50:50 ZVI/lap. mixtures, respectively (18.8 g of difference) . However, with the increase in ZVI mass to about 350 g (364.8 g and 346.5 g for the 30:70 and 50:50 granular mixtures, respectively, with 18.3 g of difference) the reactive behaviour of the 50:50 ZVI/lap. mixture was slightly better than the 30:70 ZVI/lap. mixture (Fig. 3 c-d). By increasing the ZVI mass even more (480 g and 539 g for the 30:70 and 50:50 granular mixtures, respectively) the two contaminants were even more efficiently removed by the 50:50 mixture (Fig. 3 e,-f). In this last comparison, the more efficient removal of the 50:50 mixture was likely due to the difference in iron mass between the two mixtures, which was 59 g more in the 50:50 mixture.

This second comparison confirms the influence of the ZVI content per unit volume of the reactive medium on the removal efficiency of the barrier.

250 A schematic representation of the ZVI and lapillus particles for the 50:50 and the 30:70 granular
251 mixtures, at 0.08 m and 0.18 m of column thickness, respectively, is shown in Figure 4. The ZVI
252 particles were more concentrated in the 50:50 mixture than the 30:70 mixture. The percentage of the
253 ZVI particles was 12.52% and 5.78% for the 50.50 and 30:70 granular mixtures, respectively.
254
255 *3.2 Hydraulic behaviour of ZVI/lapillus granular mixtures*
256 As depicted in Figure 5, the two mixtures were compared in terms of hydraulic conductivity. The
257 initial value of hydraulic conductivity was of $1 \cdot 10^{-4}$ m/s for both mixtures, which then decreased of
258 just over one order of magnitude for the 30:70 mixture and of four orders of magnitude for the
259 50:50 mixture.
260 As previously reported, the hydraulic conductivity reduction is linked to the ZVI content and is
261 mainly due to the expansive nature of iron corrosion products and to gas formation, and, to a lesser
262 degree, to minerals precipitation, which contributes to the removal of contaminants (Moraci et al.,
263 2016b). The greater reduction observed in the 50:50 mixture was linked to the higher ZVI content
264 per unit volume of the column (see Fig. 4), and consequently, to the higher quantity of corrosion
265 products and gases. This result was in good agreement with previous studies (Madaffari et al., 2017)
266 (Moraci et al., 2015) (Moraci et al., 2016a).
267 Thus, while the 50:50 mixture showed a better performance in terms of removal behaviour than the
268 30:70 mixture, it was less efficient than the 30:70 mixture when considering the hydraulic
269 behaviour. Therefore, the following solutions should be taken into account for a correct operation of
270 a PRB composed of ZVI and lapillus: i) if a 50:50 mixture is used, a constant monitoring of the
271 hydraulic performance of the barrier is suggested in order to provide a prompt replacement of the
272 reactive medium; ii) if a 30:70 mixture is used, a PRB thickness greater than that of the 50:50
273 mixture should be considered; iii) the possibility to adopt an intermediate weight ratio between
274 30:70 and 50:50; iv) the possibility to use a lower w.r. (for example the 30:70 w.r.) only in the first
275 3 cm of the reactive medium, because usually permeability reduction mainly occurs in the first few

276 centimetres, and use the 50:50 w.r. in the remaining part of the barrier.

277

278 *3.3 Breakthrough curves fitting*

279 In order to try to predict the reactive behaviour of the two granular mixtures and to obtain
280 parameters useful for the PRB design, the breakthrough curves were fitted through three
281 mathematical models widely used in the literature: the Thomas, the Adams-Bohart and the modified
282 dose-response model. Since adsorption can be considered the main removal mechanism for both
283 nickel and zinc the models were applied for these two contaminants. The concentration values,
284 obtained at each sampling port, were fitted to the three models using regression analyses.

285 The kinetic parameters found by applying the three models together with the values of the
286 correlation coefficient (r^2) for the 30:70 and 50:50 mixtures and for all sampling ports are listed in
287 Tables 2 and 3 for Ni and Zn, respectively. The experimental values of the equilibrium removal
288 capacity q_e calculated through equation 2, for the two mixtures and for Zn and Ni, are also shown in
289 the tables mentioned above. The q_e value was not calculated for both reactive media and for Ni at 3
290 cm of the reactive medium thickness, since, as previously observed, the typical breakthrough curve
291 was not observed at this thickness.

292 The results, obtained at 50 cm of the reactive medium thickness, for the 30:70 and the 50:50
293 ZVI/lap. mixtures, are shown in Figures 6 and 7, respectively.

294 The experimental data fitted with the three mathematical models with r^2 values, which were mostly
295 (90.3%) higher than 0.8. More specifically, the Adams-Bohart model (dash-dot line) provided the
296 highest values of the correlation coefficient, followed by the modified dose-response (continuous
297 line) and by the Thomas model (dashed line). In particular, the r^2 values were very similar for the
298 latter two models and were slightly better for the modified dose-response model when compared to
299 the experimental data (black triangle).

300 As can be observed in Figures 6 and 7a, the Thomas model did not reproduce the first part of the
301 breakthrough curve adequately, which is very important for PRB design in order to correctly

302 estimate the breakthrough time.

303 As shown in Tables 2 and 3, the experimental (q_e) and predicted values (q_{Th} and q_{mdr}) of the removal
304 capacity were generally close and, in particular, the modified dose-response model provided values
305 of the removal capacity (q_{mdr}) similar to those predicted by the Thomas model (q_{th}) and generally
306 slightly lower than the experimental values (q_e).

307 q_e values clearly reflect the breakthrough curves observed in Figures 2 and S2 highlighting the
308 higher reactivity of the 50:50 mixture compared to the 30:70 one, when the same total thickness is
309 considered. As previously mentioned Ni and Zn removal can be mainly attributed to adsorption
310 processes. The results basically confirm previous findings indicating that removal is to be mainly
311 attributed to adsoption on iron corrosion products. In fact, a lower amount of lapillus and a greater
312 amount of iron per unit volume are contained in the 50:50 column respect to the 30:70 one.
313 Furthermore, the q_e values decreased with the increase in reactive medium thickness, probably
314 because ZVI was consumed over time also by water already treated upstream, as also reported in a
315 previous work (Madaffari et al., 2017).

316

317 *3.4 Applicability of kinetic models for the prediction of column tests results*

318 The thickness and lifetime of the barrier are two fundamental parameters in PRB design (Moraci et
319 al., 2017). The mathematical models allow to predict, for a specific barrier thickness, the profile
320 over time of the C_t/C_0 ratio and, therefore, they allow to evaluate the time when the contaminant
321 concentration overcomes the regulatory limit, which represents the lifetime of the barrier when the
322 hydraulic conductivity does not decrease over time to values less than the hydraulic conductivity of
323 the aquifer.

324 The kinetic parameters derived by the application of the three models were used in order to predict
325 the estimated breakthrough time t_b at each sampling port for both reactive mediums. In each model
326 the value of C_t was placed equals to the Italian regulatory value (equals to 0.02 mg/l and 3 mg/l for
327 Ni and Zn, respectively). The results obtained are summarised in Tables 4 and 5 for the 30:70 and

328 50:50 mixtures, respectively.

329 As shown in Tables 4 and 5, the Thomas model provided negative t_b values in most cases, as can be
330 expected from the curves depicted in Figures 6 and 7 and thus it appeared unsuitable for modelling
331 in this specific case.

332 For Ni, the Adams-Bohart model gave t_b values that appeared to be unrealistic since they did not
333 increase with thickness, as expected. The modified dose-response model seemed to give slightly
334 better results, which were, however, far from the experimental values (Table 1). This may be
335 explained by the fact that the regulatory limit was 0.04% of the initial concentration used in this
336 study making it difficult to correctly assess the breakthrough occurrence. Therefore, the three
337 models were not adequate to accurately predict the reactive behaviour of the two granular mixtures.

338 For Zn, the Adams-Bohart model adequately fitted the experimental values while the other two
339 models tended to underestimate the breakthrough time, as can be observed by comparing the
340 experimental values summarised in Table 1 with those presented in Tables 4 and 5 (in this case the
341 regulatory limit was 6% of the initial concentration).

342 Therefore, in order to predict the thickness and lifetime of a barrier designed for Zn removal, we
343 proposed two methods using the Adams-Bohart equation based on the assumption that the hydraulic
344 conductivity did not decrease significantly over time.

345 The first method consisted of plotting the Zn breakthrough time ($t_{A\text{-}B}$) as a function of barrier
346 thickness (T) and to fit the values through a power function (e.g. $y = a \cdot X^b$) for the two mixtures, as
347 shown in Figure 8.

348 As can be observed in Figure 8, the barrier thickness, necessary to reduce Zn concentration below
349 the regulatory limit, increased over time for the two mixtures according to a power function
350 ($r^2 \geq 0.91$), which had a similar value of the exponent (0.60 and 0.64 for the 30:70 and 50:50 mixture,
351 respectively).

352 The power function could allow to predict the reactive behaviour of the reactive medium during the
353 design phase for thicknesses greater than 0.5 m.

354 The second method allowed to estimate the kinetic parameters (K_{AB} and N_0) for different values of
355 the barrier thickness. It consisted of plotting the kinetic parameters, normalised to the barrier
356 thickness, as a function of the barrier thickness (T), and to fit the values through a power function,
357 for the 30:70 and 50:50 granular mixtures, respectively, as shown in Figures 9 and 10. In order to
358 obtain the maximum value of r^2 the kinetic parameters of the Adams-Bohart model (K_{AB} and N_o)
359 referring to 3 cm were eliminated for both mixtures. The data were well fitted with r^2 values higher
360 than 0.987.
361 The power function could allow to predict the kinetic parameters, of the Adams-Bohart model, for
362 thicknesses greater than 0.5 m and, subsequently, through eq. 4 it is possible to estimate the time t
363 at which the contaminant concentration C_t complied with the regulatory limit to be guaranteed
364 downstream of the barrier (i.e. t_b).
365 In Table 6 the t_b values were determined for thicknesses greater than 50 cm using the first (power
366 equations in Figure 8) and second method (power equations in Figures 9 and 10).
367 The t_b values determined with the second method proposed provided values, which were slightly
368 more conservative than the first method although both were in very good agreement. It is necessary
369 to underline that the accuracy of the two proposed methods is strictly linked to the equations used to
370 fit the data, especially the equations used to fit the kinetic parameter values (i.e. K_{AB}) due to the low
371 and similar values.
372
373 **4. Conclusions**
374 This study shows the potential use of the ZVI/lapillus mixtures at two different weight ratios (i.e.
375 30.70 and 50:50) for the removal, through PRB technology, of Cu, Ni and Zn from pluri-
376 contaminated solutions. The major findings derived from this study are summarised as follows:
377 1. Heavy metals were removed according to the following sequence: Cu>Zn>Ni.
378 2. The ZVI/lapillus mixture at higher iron content (50:50) showed the higher removal rate but
379 also the higher reduction of hydraulic conductivity in the long run.

3. For a correct hydraulic operation of the 50:50 granular mixture, a constant monitoring of its hydraulic performance is required in order to provide a prompt replacement of the reactive medium; alternatively, the following options should be further investigated: i) adopt a 30:70 granular mixture with a thickness greater than that investigated in this study; ii) adopt an intermediate weight ratio between 30:70 and 50:50; iii) use a lower w.r. (for example the 30:70 w.r.) only in the first 3 cm, because usually permeability reduction occurs mainly in the first centimetres of the reactive medium, and use the 50:50 w.r. in the remaining part of the barrier.
4. The experimental data were fitted with three mathematical models: the Thomas, the Adams-Bohart and the modified dose-response model. The Adams-Bohart model provided the best fit and the highest values of the correlation coefficient (r^2).
5. The applicability of these models was evaluated for the PRB design. None of the three models was adequate to accurately predict Ni breakthrough, whereas for Zn only the Adams-Bohart model was able to accurately predict the breakthrough time. Therefore, two methods were proposed, by using the latter model, in order to predict the Zn removal front along the barrier thickness.

Acknowledgements

All the authors contributed in an equal manner to the present paper. This research was funded by the Italian Ministry of Education, University and Research [Ministero dell'Istruzione, dell'Università e della Ricerca] within the Project PON01_01869TEMADITUTELA.

References

Bartzas, G., Komnitsas, K., 2010. Solid phase studies and geochemical modelling of low-cost permeable reactive barriers. J. Hazard. Mater. 183, 301–8. https://doi.org/10.1016/j.jhazmat.2010.07.024

Bilardi, S., Calabrò, P.S., Caré, S., Moraci, N., Noubactep, C., 2013. Improving the sustainability of

granular iron/pumice systems for water treatment. J. Environ. Manage. 121. https://doi.org/10.1016/j.jenvman.2013.02.042

Bilardi, S., Calabró, P.S., Moraci, N., 2015. Simultaneous removal of CU^{II}, NI^{II} and ZN^{II} by a granular mixture of zero-valent iron and pumice in column systems. Desalin. Water Treat. 55. https://doi.org/10.1080/19443994.2014.916234

Bilardi, S., Calabrò, P.S., Moraci, N., Madaffari, M.G., Ranjbar, E., 2018. A Comparison between Fe0/Pumice and Fe0/Lapillus Mixtures in Permeable Reactive Barriers. Environ. Geotech. 1–52. https://doi.org/10.1680/jenge.17.00095

Bohart, G.S., Adams, E.Q., 1920. Some aspects of the behavior of charcoal with respect to chlorine. J. Am. Chem. Soc. 42, 523–544. https://doi.org/10.1021/ja01448a018

Cundy, A.B., Hopkinson, L., Whitby, R.L.D., 2008. Use of iron-based technologies in contaminated land and groundwater remediation: a review. Sci. Total Environ. 400, 42–51. https://doi.org/10.1016/j.scitotenv.2008.07.002

de Franco, M.A.E., de Carvalho, C.B., Bonetto, M.M., Soares, R. de P., Féris, L.A., 2017. Removal of amoxicillin from water by adsorption onto activated carbon in batch process and fixed bed column: Kinetics, isotherms, experimental design and breakthrough curves modelling. J. Clean. Prod. 161, 947–956. https://doi.org/10.1016/J.JCLEPRO.2017.05.197

EPA, 1999. Field Applications of In Situ Remediation Technologies: Permeable Reactive Barriers. Washington DC.

Fu, F.L., Dionysiou, D.D., Liu, H., 2014. The use of zero-valent iron for groundwater remediation and wastewater treatment: A review. J. Hazard. Mater. 267, 194–205. https://doi.org/10.1016/j.jhazmat.2013.12.062

Hashim, M.A., Mukhopadhyay, S., Sahu, J.N., Sengupta, B., 2011. Remediation technologies for heavy metal contaminated groundwater. J. Environ. Manage. https://doi.org/10.1016/j.jenvman.2011.06.009

Huang, D., Wang, G., Shi, Z., Li, Z., Kang, F., Liu, F., 2017. Removal of hexavalent chromium in natural groundwater using activated carbon and cast iron combined system. J. Clean. Prod. 165, 667–676. https://doi.org/10.1016/J.JCLEPRO.2017.07.152

Komnitsas, K., 2007. Long-term efficiency and kinetic evaluation of ZVI barriers during clean-up of copper containing solutions 20, 1200–1209. https://doi.org/10.1016/j.mineng.2007.05.002

Lin, S., Liu, L., Yang, Y., Lin, K., 2017. Study on preferential adsorption of cationic-style heavy metals using amine-functionalized magnetic iron oxide nanoparticles (MIONPs-NH2) as efficient adsorbents. Appl. Surf. Sci. 407, 29–35.

441 https://doi.org/10.1016/J.APSUSC.2017.02.173
442 Madaffari, M.G., Bilardi, S., Calabrò, P.S., Moraci, N., 2017. Nickel removal by zero valent
443 iron/lapillus mixtures in column systems. Soils Found. 57.
444 https://doi.org/10.1016/j.sandf.2017.08.006
445 Mikhaylov, V.I., Maslennikova, T.P., Krivoshapkina, E.F., Tropnikov, E.M., Krivoshapkin, P. V.,
446 2018. Express Al/Fe oxide–oxyhydroxide sorbent systems for Cr(VI) removal from aqueous
447 solutions. Chem. Eng. J. https://doi.org/10.1016/j.cej.2018.05.023
448 Moraci, N., Bilardi, S., Calabrò, P.S., 2017. Fe0/pumice mixtures: From laboratory tests to
449 permeable reactive barrier design. Environ. Geotech. 4. https://doi.org/10.1680/jenge.15.00002
450 Moraci, N., Bilardi, S., Calabrò, P.S., 2016a. Critical aspects related to Fe^0 and Fe^0/pumice PRB
451 design. Environ. Geotech. 3. https://doi.org/10.1680/envgeo.13.00120
452 Moraci, N., Bilardi, S., Calabrò, P.S., 2015. Design of permeable reactive barriers for remediation
453 of groundwater contaminated by heavy metals. Riv. Ital. di Geotec. 49.
454 Moraci, N., Calabrò, P.S., 2010. Heavy metals removal and hydraulic performance in zero-valent
455 iron/pumice permeable reactive barriers. J. Environ. Manage. 91, 2336–2341.
456 https://doi.org/10.1016/j.jenvman.2010.06.019
457 Moraci, N., Calabrò, P.S., Suraci, P., 2011. Long-term efficiency of Zero-Valent iron - Pumice
458 Granular mixtures for the removal of Copper or Nickel from groundwater. Soils and Rocks 34,
459 129–138.
460 Moraci, N., Ielo, D., Bilardi, S., Calabro, P.S., 2016b. Modelling long-term hydraulic conductivity
461 behaviour of zero valent iron column tests for permeable reactive barrier design. Can. Geotech.
462 J. 53. https://doi.org/10.1139/cgj-2015-0453
463 Noubactep, C., 2013. Metallic Iron for Water Treatment: A Critical Review. CLEAN - Soil, Air,
464 Water 41, 702–710. https://doi.org/10.1002/clen.201200502
465 Obiri-Nyarko, F., Grajales-Mesa, S.J., Malina, G., 2014. An overview of permeable reactive
466 barriers for in situ sustainable groundwater remediation. Chemosphere.
467 https://doi.org/10.1016/j.chemosphere.2014.03.112
468 President of the Italian Republic, 2006. d.lgs. n. 152/2006 (T.U. ambiente) [WWW Document].
469 URL http://www.bosettiegatti.eu/info/norme/statali/2006_0152.htm (accessed 1.24.19).
470 Shanmugam, D., Alagappan, M., Rajan, R.K., 2016. Bench-scale packed bed sorption of Cibacron
471 blue F3GA using lucrative algal biomass. Alexandria Eng. J. 55, 2995–3003.
472 https://doi.org/10.1016/J.AEJ.2016.05.012
473 Singh, D.K., Kumar, V., Mohan, S., Bano, D., Hasan, S.H., 2017. Breakthrough curve modeling of
474 graphene oxide aerogel packed fixed bed column for the removal of Cr(VI) from water. J.

475 Water Process Eng. 18, 150–158. https://doi.org/10.1016/J.JWPE.2017.06.011
476 Sulaymon, A.H., Faisal, A.A.H., Khaliefa, Q.M., 2015. Cement kiln dust (CKD)-filter sand
477 permeable reactive barrier for the removal of Cu(II) and Zn(II) from simulated acidic
478 groundwater. J. Hazard. Mater. 297, 160–172. https://doi.org/10.1016/j.jhazmat.2015.04.061
479 Thomas, H.C., 1948. CHROMATOGRAPHY: A PROBLEM IN KINETICS. Ann. N. Y. Acad. Sci.
480 49, 161–182. https://doi.org/10.1111/j.1749-6632.1948.tb35248.x
481 USEPA, 1989. EVALUATION OF GROUNDWATER EXTRACTION REMEDIES - VOLUME
482 II.
483 Yan, G., Viraraghavan, T., Chen, M., 2001. A New Model for Heavy Metal Removal in a
484 Biosorption Column. Adsorpt. Sci. Technol. 19, 25–43.
485 https://doi.org/10.1260/0263617011493953
486

Table
Click here to download Table: Tables.docx

Table 1: Breakthrough time (t_b) of Ni and Zn, for the ZVI/lapillus mixtures at different thicknesses (T), and mass of ZVI and lapillus.

ZVI/lap. 30:70 w.r.					**ZVI/lap. 50:50 w.r.**				
T [cm]	lap. [g]	ZVI [g]	t_b [h] Ni	Zn	T [cm]	lap. [g]	ZVI [g]	t_b [h] Ni	Zn
3	67.2	28.8	0	240	3	57.75	57.75	0	600
8	179.2	76.8	240	432	8	154	154	432	912
18	403.2	172.8	432	744	18	346.5	346.5	432	1272
28	627.2	268.8	432	912	28	539	539	744	2112
38	851.2	364.8	432	1272	38	731.5	731.5	1032	2112
50	1120	480	600	1272	50	962.5	962.5	1032	2880

Table 2: Kinetic model parameters and the equilibrium removal capacity q_e for Ni removal at different thicknesses of the ZVI/lap. mixtures.

ZVI/lap. 30:70		**Thomas model**			**Adams-Bohart model**			**modified dose-response model**		
T cm	q_e mg/g	k_{Th} L/(mg·h)	q_{Th} mg/g	r^2	K_{AB} L/(mg·h)	N_0 mg/L	r^2	a	q_{mdr} mg/g	r^2
3	-	1.42	0.86	0.73	$1.00\cdot10^{-4}$	5747.95	0.99	16.01	0.88	0.73
8	2.17	$2.33\cdot10^{-4}$	2.28	0.87	$2.06\cdot10^{-3}$	2486.80	0.99	4.54	2.20	0.87
18	1.7	$3.59\cdot10^{-4}$	1.45	0.95	$1.86\cdot10^{-3}$	1980.36	0.99	7.68	1.45	0.96
28	1.63	$7.31\cdot10^{-5}$	1.36	0.93	$3.72\cdot10^{-4}$	1756.38	0.99	2.81	1.26	0.96
38	1.55	$6.36\cdot10^{-5}$	1.17	0.86	$2.70\cdot10^{-4}$	1457.68	0.99	2.54	1.11	0.91
50	1.13	$7.09\cdot10^{-5}$	0.94	0.93	$2.13\cdot10^{-4}$	1247.62	0.99	3.40	0.89	0.95
ZVI/lap. 50:50										
3	1.83	$1.22\cdot10^{-4}$	1.62	0.81	$7.10\cdot10^{-5}$	8420.24	0.99	1.40	1.16	0.76
8	2.79	$2.41\cdot10^{-4}$	3.30	0.97	$2.34\cdot10^{-4}$	6661.32	0.99	8.38	3.26	0.97
18	2.72	$9.26\cdot10^{-5}$	2.44	0.98	$1.59\cdot10^{-4}$	4590.74	0.95	4.79	2.39	0.99
28	2.41	$5.62\cdot10^{-5}$	2.31	0.97	$2.95\cdot10^{-4}$	3077.54	0.99	4.10	2.25	0.98
38	2.06	$6.12\cdot10^{-5}$	2.01	0.98	$8.66\cdot10^{-5}$	3812.32	0.99	5.47	1.97	0.99
50	1.79	$5.27\cdot10^{-5}$	1.80	0.98	$6.86\cdot10^{-5}$	3570.06	0.98	5.57	1.76	0.99

Table 3: Kinetic model parameters and the equilibrium adsorption capacity q_e for Zn removal at different thicknesses of the ZVI/lap. mixtures.

ZVI/lap. 30:70		**Thomas model**			**Adams-Bohart model**			**modified dose-response model**		
T cm	q_e mg/g	k_{Th} L/(mg·h)	q_{Th} mg/g	r^2	K_{AB} L/(mg·h)	N_0 mg/L	r^2	a	q_{mdr} mg/g	r^2
3	3.78	$3.82\cdot10^{-4}$	3.44	0.98	$2.10\cdot10^{-3}$	6235.84	0.99	3.76	3.36	0.98
8	3.53	$1.75\cdot10^{-4}$	3.64	0.86	$2.69\cdot10^{-4}$	6187.80	0.99	5.32	3.58	0.87
18	3.01	$7.87\cdot10^{-5}$	2.59	0.92	$1.03\cdot10^{-4}$	4319.25	0.88	3.41	2.47	0.94
28	3.00	$6.07\cdot10^{-5}$	2.42	0.92	$1.30\cdot10^{-4}$	3925.02	0.99	3.36	2.35	0.95
38	2.86	$3.95\cdot10^{-5}$	2.28	0.86	$1.06\cdot10^{-4}$	3256.11	0.99	2.78	2.23	0.92
50	2.01	$3.66\cdot10^{-5}$	2.14	0.97	$7.59\cdot10^{-5}$	2870.57	0.94	3.60	2.06	0.99
ZVI/lap. 50:50										
3	-	$1.66\cdot10^{-4}$	9.10	0.85	$2.97\cdot10^{-4}$	17302.8	0.99	5.52	8.95	0.85
8	6.78	$4.41\cdot10^{-5}$	5.67	0.56	$6.66\cdot10^{-4}$	8773.88	0.99	2.05	5.38	0.67
18	4.56	$1.74\cdot10^{-5}$	6.25	0.46	$1.70\cdot10^{-4}$	6268.16	0.99	1.52	6.14	0.59
28	3.59	$2.76\cdot10^{-5}$	4.75	0.85	$1.19\cdot10^{-4}$	6385.20	0.99	3.01	5.04	0.90

38	2.95	$3.63 \cdot 10^{-5}$	3.48	0.85	$7.79 \cdot 10^{-5}$	5703.94	0.99	4.44	3.60	0.97
50	2.35	$4.24 \cdot 10^{-5}$	2.89	0.90	$8.33 \cdot 10^{-5}$	4981.59	0.96	5.87	3.00	0.91

Table 4: Ni and Zn estimated breakthrough time (h) calculated by means of the Thomas (t_T), Adams-Bohart (t_{A-B}) and modified dose-response (t_{md-r}) models for the 30:70 mixture.

	Nickel			**Zinc**		
T [cm]	t_T [h]	t_{A-B} [h]	t_{md-r} [h]	t_T [h]	t_{A-B} [h]	t_{md-r} [h]
3	54.89	-	46.61	75.97	217.94	52.59
8	-	184.16	196.42	307.66	438.31	103.23
18	121.06	382.43	379.09	293.74	468.90	257.68
28	-	223.26	264.16	538.59	1004.81	386.93
38	-	145.87	282.47	454.66	1088.48	609.01
50	-	81.59	398.60	772.40	1136.86	563.45

- the model gives a negative value

Table 5: Ni and Zn estimated breakthrough time (h) calculated by means of the Thomas (t_T), Adams-Bohart (t_{A-B}) and modified dose-response (t_{md-r}) models for the 50:50 mixture.

	Nickel			**Zinc**		
T [cm]	t_T [h]	t_{A-B} [h]	t_{md-r} [h]	t_T [h]	t_{A-B} [h]	t_{md-r} [h]
3	-	-	0.34	369.51	489.53	418.89
8	27.24	29.14	263.20	-	833.850	288.63
18	-	97.91	215.69	-	1144.49	465.90
28	-	597.30	240.31	1419.24	1866.67	1452.47
38	-	88.41	459.00	1875.68	2113.68	1888.11
50	-	55.68	553.35	2407.66	2583.35	2412.9

- the model gives a negative value

Table 6: Zn estimated breakthrough time t_b (days) for the 30:70 and 50:50 mixtures using the first and the second method.

T [m]	ZVI/lap. 30:70 w.r.		ZVI/lap. 50:50 w.r.	
	1° method	2° method	1° method	2° method
0.6	58.36	53.04	120.12	116.48
0.8	69.53	61.81	144.61	135.80
1	79.64	69.54	167.00	151.80

Figure
Click here to download Figure: Figures.docx

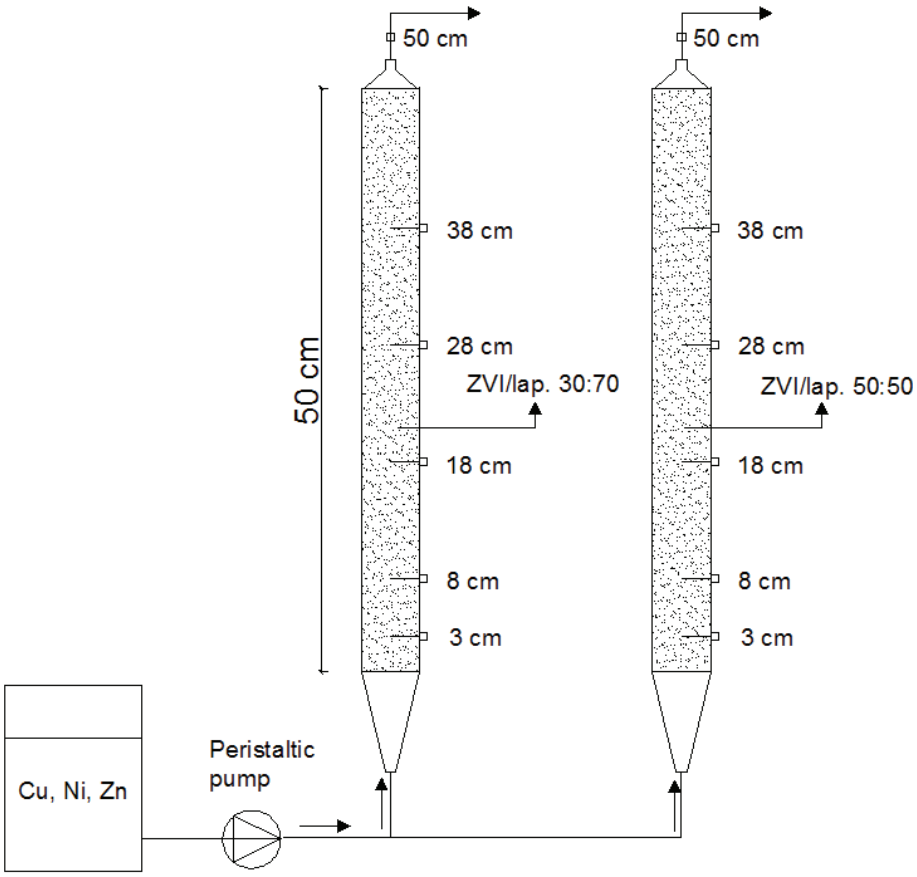

Figure 1: Schematic diagram of the column tests

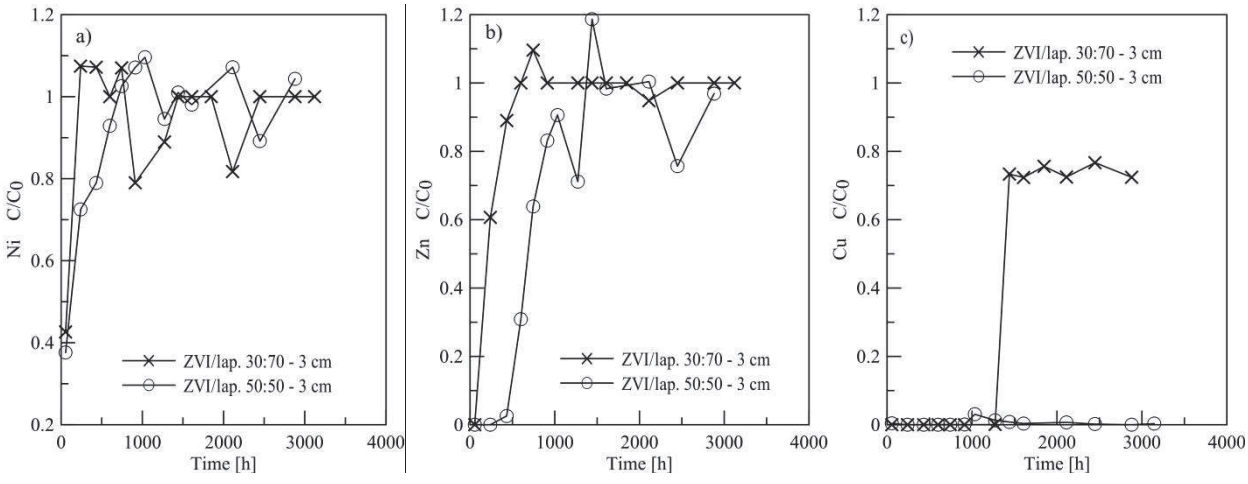

Figure 2: Ni, Zn and Cu breakthrough curves at 3 cm of the ZVI/lap. mixtures

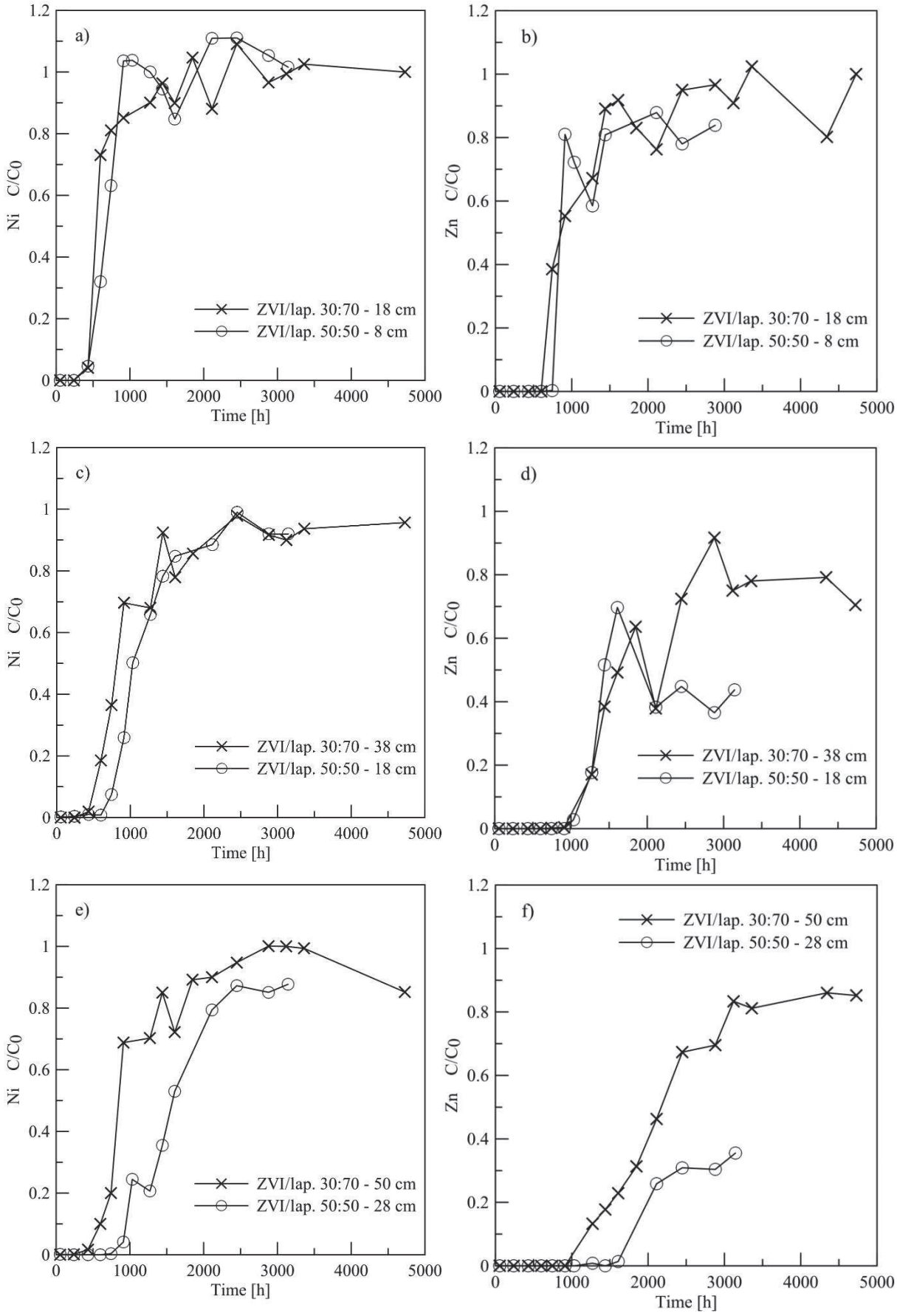

Figure 3: Ni and Zn breakthrough curves for the ZVI/lap. mixtures considering different reactive medium thicknesses

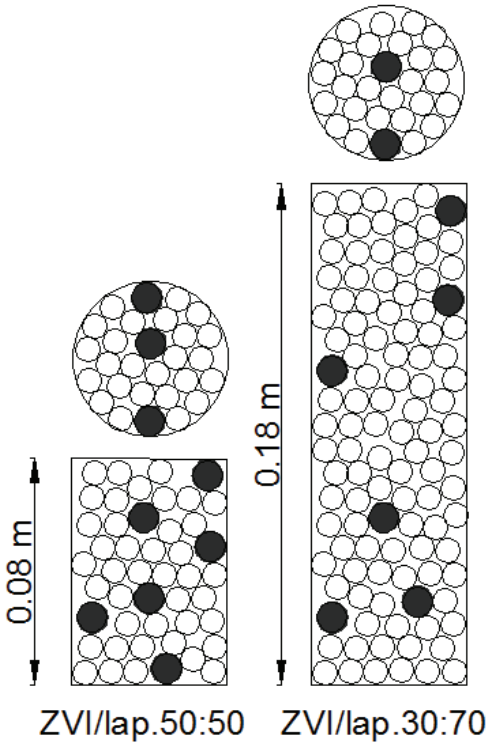

Figure 4: Schematic representation of the ZVI (full circles) and lapillus particles (empty circles) considering thicknesses of 0.08 m and 0.18 m for the 50:50 and 30:70 granular mixtures, respectively

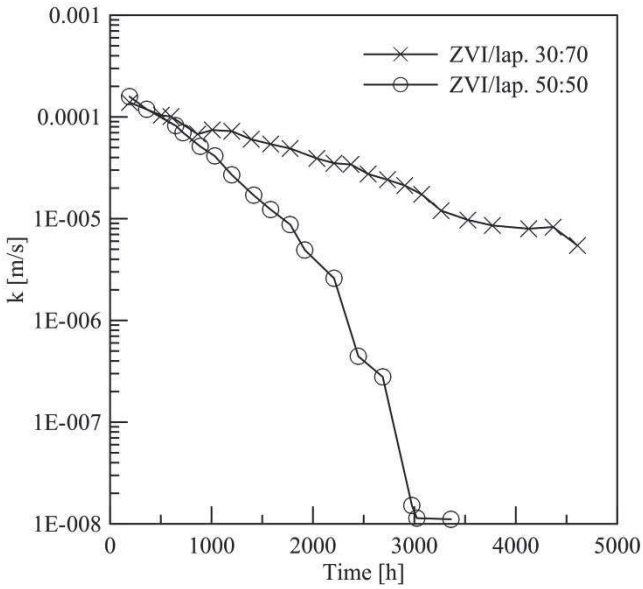

Figure 5: Hydraulic conductivity versus time for the ZVI/lap. mixtures at 30:70 and 50:50 w.r.

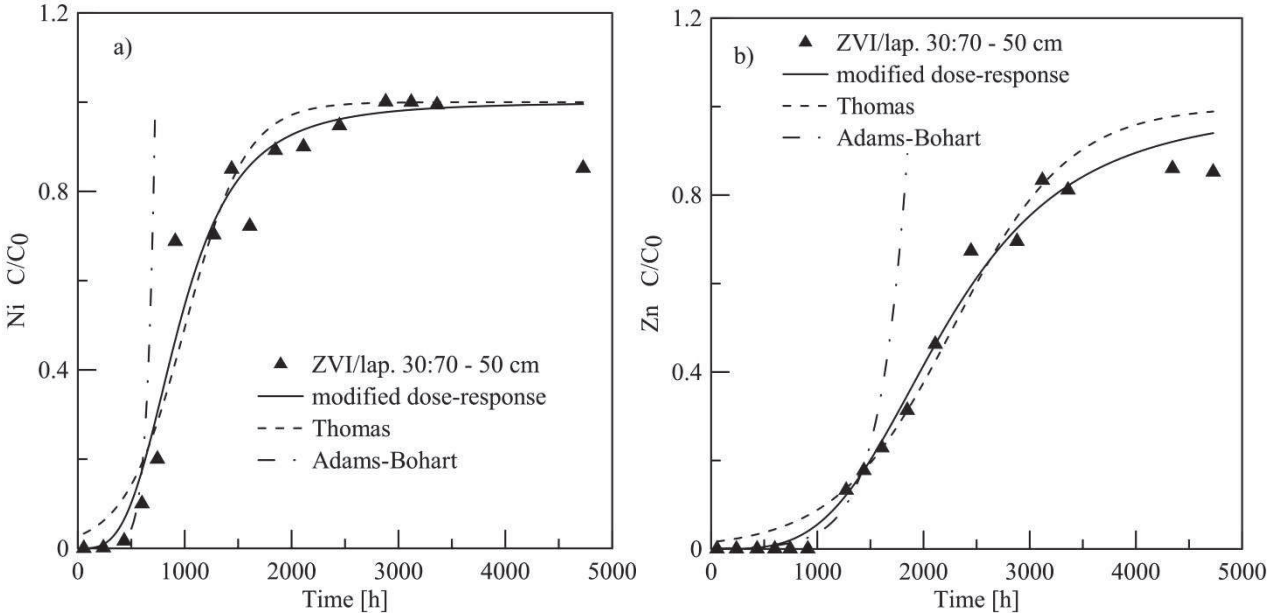

Figure 6: The experimental and predicted data using the Thomas, Adams-Bohart and modified dose -response models for a) Ni and b) Zn of the 30:70 ZVI/lap. mixture

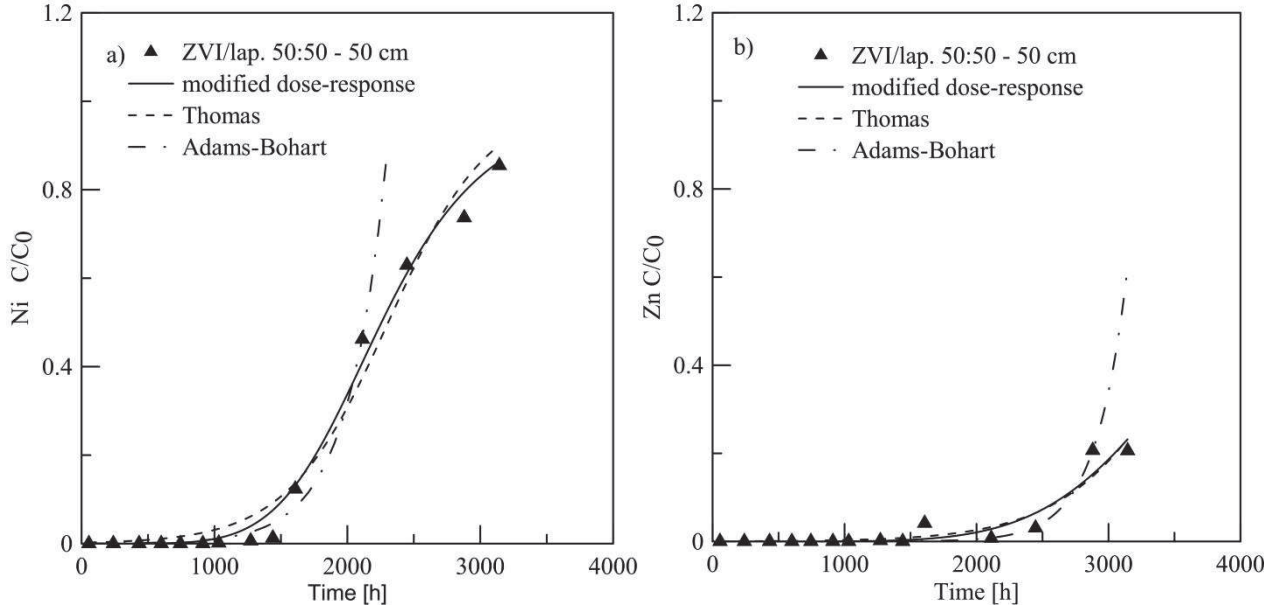

Figure 7: The experimental and predicted data using the Thomas, Adams-Bohart and modified dose-response models for a) Ni and b) Zn of the 50:50 ZVI/lap. mixture

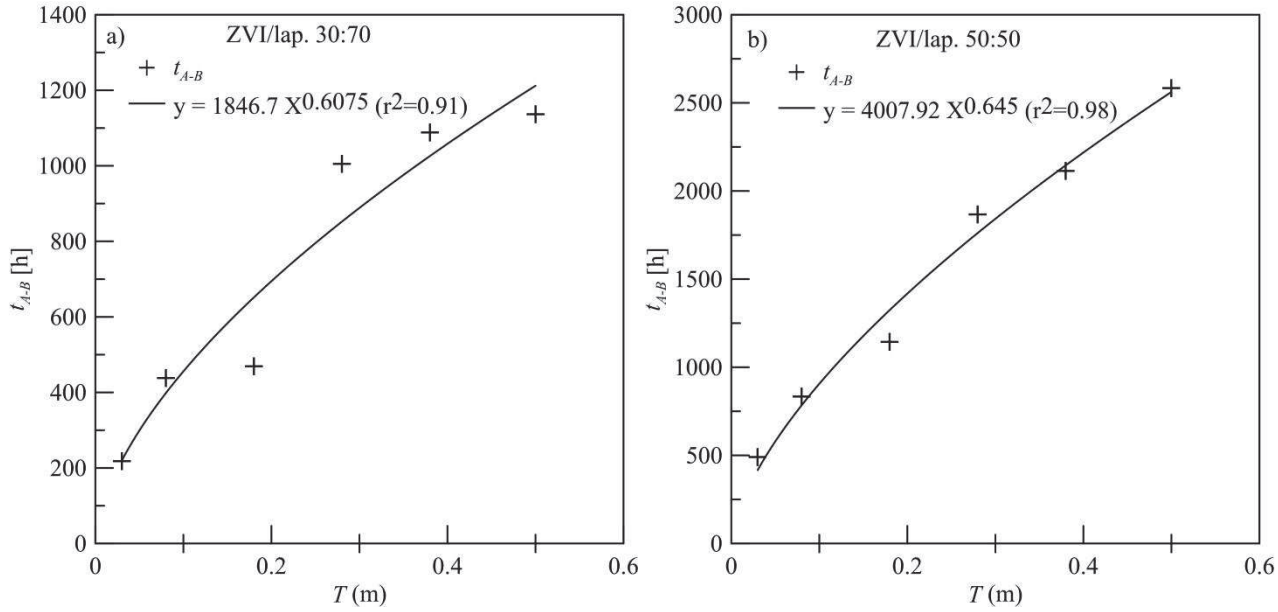

Figure 8: The t_{A-B} (h) values versus T (m) for the ZVI/lap. mixture at a) 30:70 and b) 50:50 w.r.

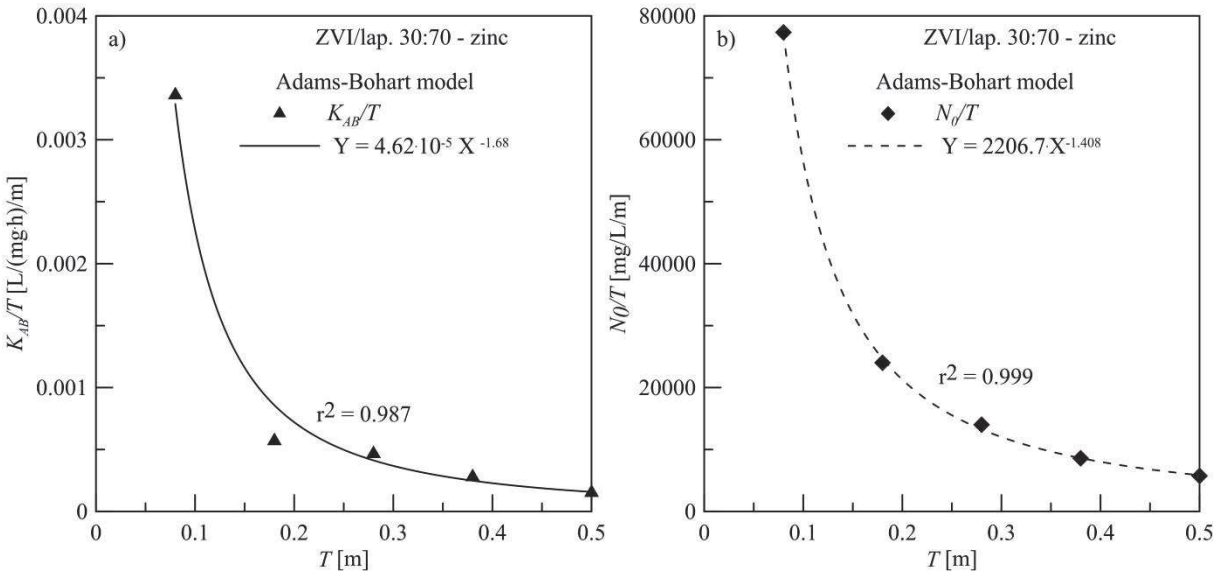

Figure 9: The normalised values of the kinetic parameters of the Adams-Bohart model for the 30:70 mixture

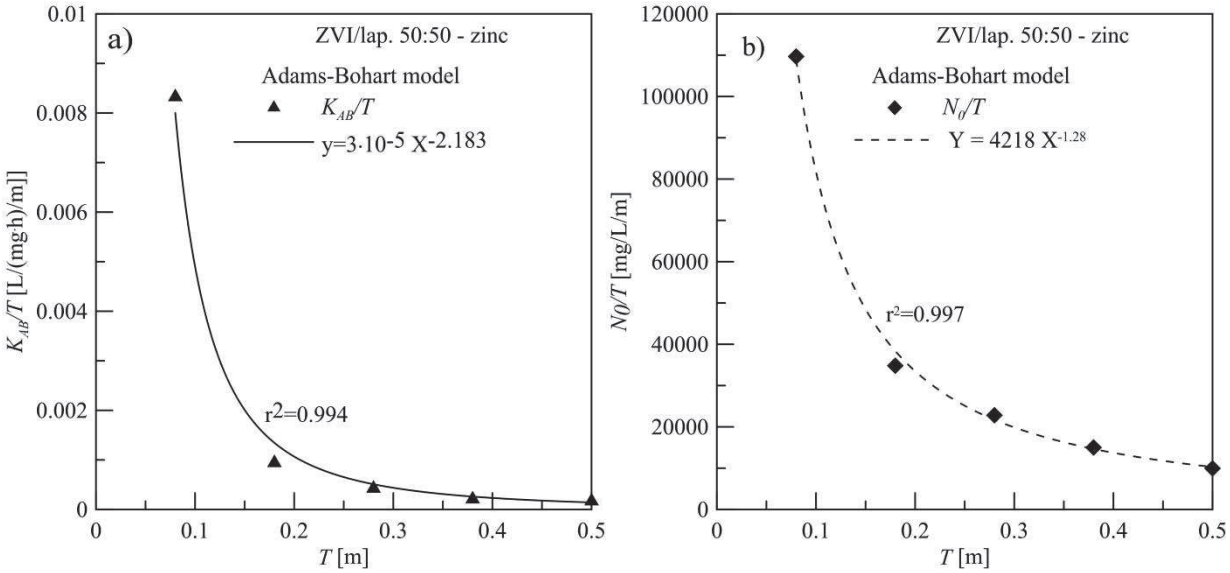

Figure 10: The normalised values of the kinetic parameters of the Adams-Bohart model for the 50:50 mixture

Supplementary material for on-line publication only

Click here to download Supplementary material for on-line publication only: Supplementary material.docx